Electronic Supplementary Material (ESI) for Physical Chemistry Chemical Physics.

Supporting Information :
Unraveling the Ce^{3+} detection at the surface of ceria nanopowders by UPS analysis

Luis Cardenas, Clément Molinet, and Stéphane Loridant**

Univ Lyon, Université Claude Bernard-Lyon 1, CNRS, IRCELYON-UMR 5256, 2 av. A. Einstein, F-69626 Villeurbanne Cedex, France

Corresponding Authors

*E-mail: luis.cardenas@ircelyon.univ-lyon1.fr

*E-mail: stephane.loridant@ircelyon.univ-lyon1.fr

TABLE OF CONTENTS:

1. UPS AND XPS ANALYSIS

Ultraviolet Photoelectron Spectroscopy (UPS) has been widely used to characterize a myriad of materials via their valence band. However, almost all of these UPS studies conducted have been limited to oriented single crystals. The morphology and the chemical environment generally prevent UPS's development as a characterization technique on powder catalysts. Multiple electronic interactions and charging effects often hinder an in-depth analysis of the electronic structure of nanopowders. Charge effects are generally associated with instrumentation-related issues. However, electron transport at the surface is a critical parameter associated with the material morphology and electronic structure, often neglected. Therefore, performing PES analysis on powders can be a delicate task, as it combines morphology and exotic electron behavior issues. The charging phenomenon arises from photon-electron interaction, generating an excess of positive charge (hole) at the surface. Electron transport depends on the analyzer $\emptyset_A$ and samples $\emptyset_S$ work functions. If $\emptyset_A \neq \emptyset_S$, a surface charge variance is established at the surface. This charge variance prevents then the electron correlation with their catalytic performances. Therefore, new methodologies to analyze the electronic structure of nanopowders by UPS are required to improve the catalytic performances and properly design new catalysts.

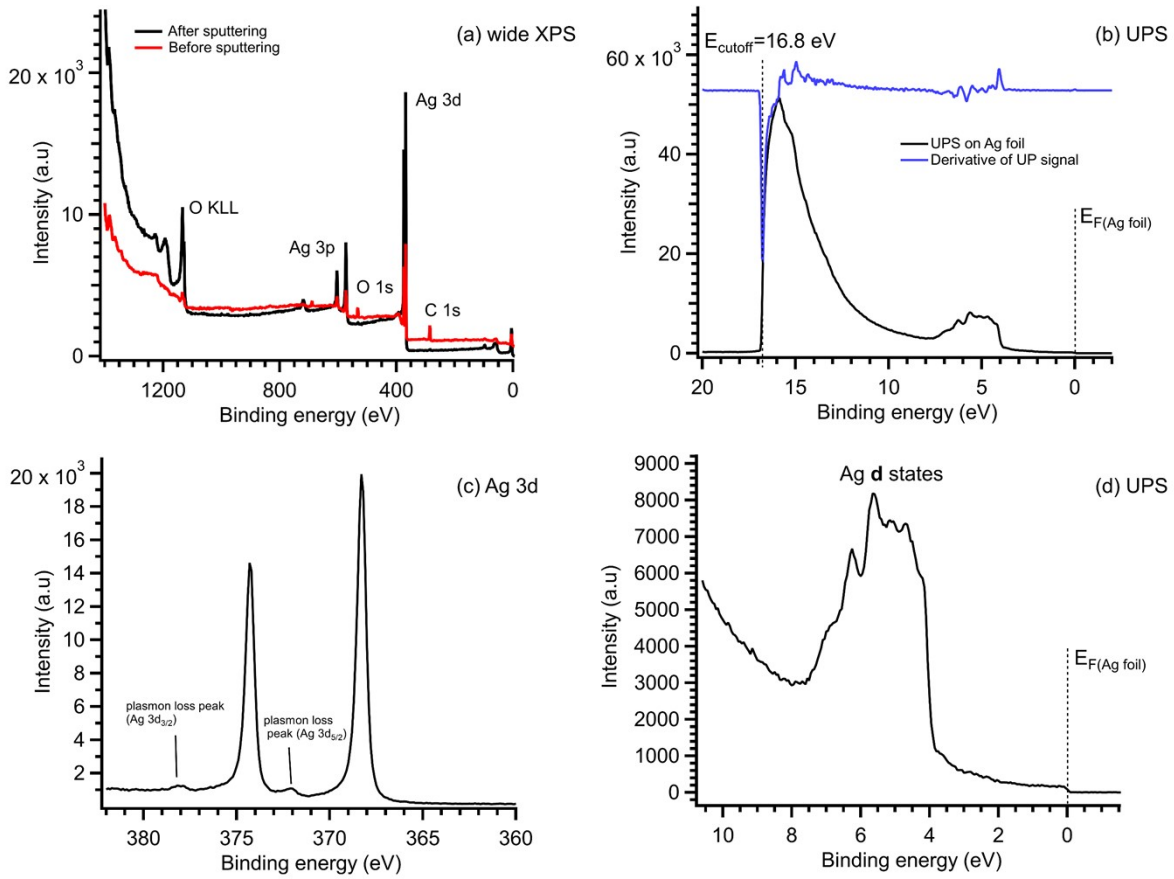

Figure S1: (a) Full wide XPS spectra of Ag foil before and after sputtering (clean). (b) Wide He I UP spectrum of the clean Ag foil (black) and its first derivative (bleu). The spectrum was acquired with a pass energy of 5 eV, an acquisition step of 0.05 eV, and a dwell time of 200 ms. The cutoff was measured at 16.8 eV by the first derivative of UP spectrum, Wf = 21.2 eV–16.8 eV =4.4 eV, within the range of values (4.2 and 4.8 eV) expected for Ag.[S1, S2] (c) XPS Ag 3d spectrum of the Ag foil ion sputtering at 3 keV. The Ag 3d spectrum exhibits plasmon contributions only visible when Ag foil is clean.[S3] (d) High-resolution UP spectrum on Ag foil with the Fermi edge.

a) **Background subtraction:**

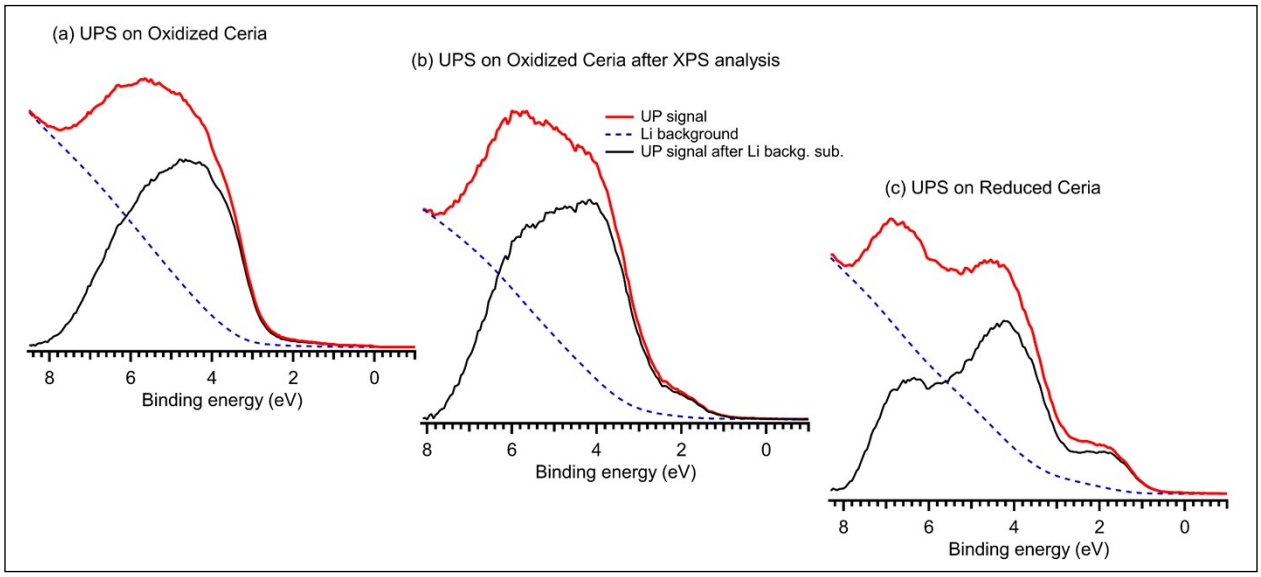

Figure S2: He I UP spectrum of: (a) oxidized ceria, (b) oxidized ceria after XPS analysis and (c) reduced ceria. All samples were prepared by drop-casting method on Ag foil (red). The background of each spectrum was subtracted using the *Li function,*[S4] which was specially developed to describe secondary-electron cascade processes as those observed in UPS.

b) **UPS Contributions:**

UPS after XPS analysis		UPS after reduction	
State	Area	State	Area
Ce 4f	0.120	Ce 4f	0.391
O 2p (1)	0.926	O 2p (1)	1.350
O 2p (2)	0.779	O 2p (2)	0.905
O 2p (3)	0.619	O 2p (3)	0.980

Table S1: Fit area of UPS spectra after pre-oxidation (left) and reduction (right) corresponding to Ce 4f and O 2p levels.

2. XRD AND TPR ANALYSIS:

a) X-RAY DIFFRACTION (XRD):

A XRD diffractogram of CeO_2 powder was recorded using a D8 Advance 25 (Bruker) diffractometer. The X-ray source, used with a power of 1.75 kW, was composed of a tungsten cathode and a copper anode. The Kα ray of Cu was selected with a Ni filter. The acquisition conditions were as follows: from 4° to 80° with a step of 0.02047° and 0.5 s of counting per step. The crystallite size was

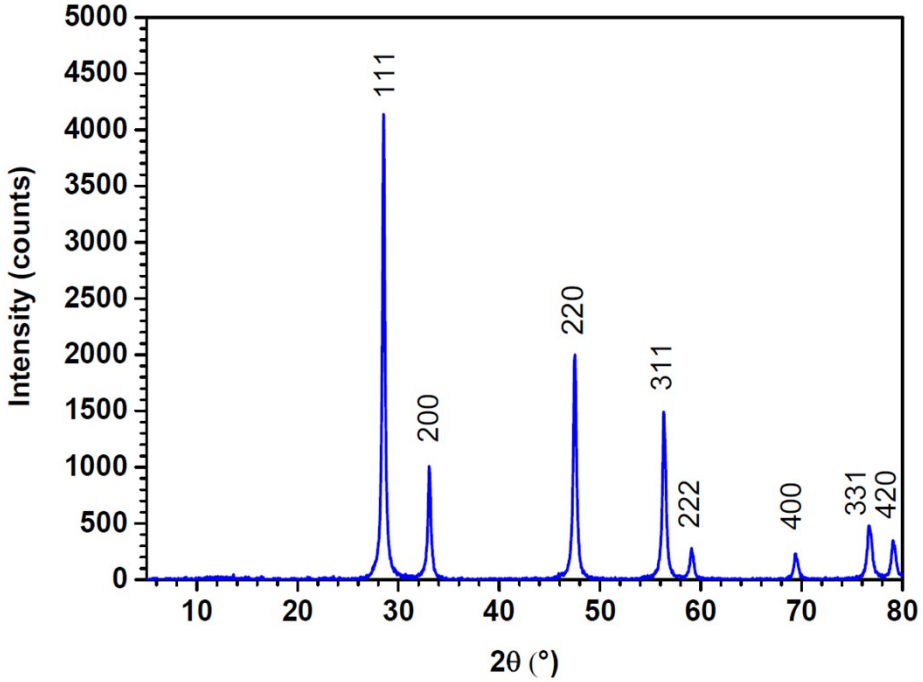

determined by measuring the width at half maximum of bands and using the following Scherrer:

Figure S3: Diffractogram of ceria powder after calcination at 600 °C during 4 h. The crystallite size determined using the Scherrer equation[S5] from the FWHM of the (111) , (200), and (220) peaks was 32 nm.

Equation: $\frac{K \times \lambda}{\sqrt{(FWHM)^2 - 0.06^2} \times cos(\theta)}$ with the constant K = 0.9, λ le wavelength of the $K_{\alpha 2}$ line (0.154184 nm), FWHM the full width at half maximum of the peak at θ corrected of the instrumental width (0.06°).[S5]

b) TEMPERATURE PROGRAMMED REDUCTION (TPR)

The reducibility of CeO_2 powder was determined by TPR measurements using a 9 Omnistar GSD 301 Pfeiffer Vacuum mass spectrometer. The dried sample (100 mg) was loaded into a suitable reactor and heated from room temperature to 600 °C (10 °C min^{-1}) for 4 h under 1%O_2/He to pre-treated CeO_2 and then cooled down to room temperature. Then, it was heated from room temperature up to 650 °C (10 °C min^{-1}) under 1% H_2-Ar.

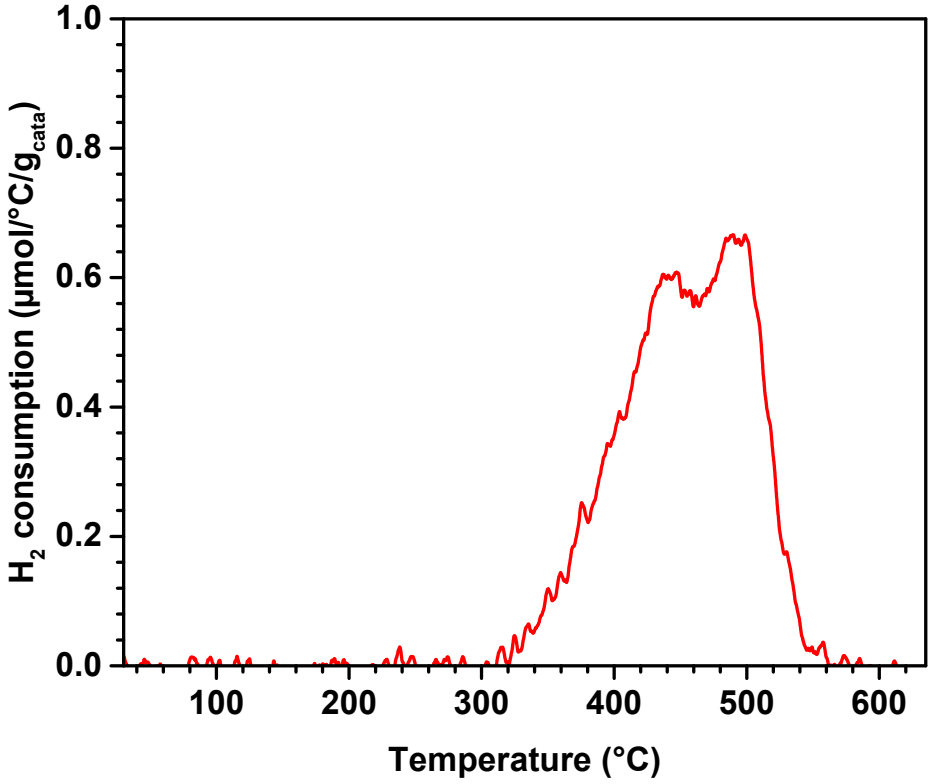

Figure S4: TPR curve of CeO_2 under 1%H_2/He flow after calcination at 600 °C during 4 h under 1%O_2/He. It contains two peaks of reduction at 444 and 490 °C, which are due to the reduction of surface ceria.[S6] The total hydrogen consumption up to 600 °C gives the stoichiometry $CeO_{(2-0.0142)}$, which corresponds to 2.8% of Ce^{3+}.

3. REFERENCES

(S1) Maheu, C.; Cardenas, L.; Puzenat, E.; Afanasiev, P.; Geantet, C. UPS and UV Spectroscopies Combined to Position the Energy Levels of TiO_2 Anatase and Rutile Nanopowders. *Phys. Chem. Chem. Phys.* **2018**, *20* (40), 25629–25637. https://doi.org/10.1039/C8CP04614J.

(S2) Derry, G. N.; Kern, M. E.; Worth, E. H. Recommended Values of Clean Metal Surface Work Functions. *J. Vac. Sci. Technol. A* **2015**, *33* (6), 060801. https://doi.org/10.1116/1.4934685.

(S3) Leiro, J.; Minni, E.; Suoninen, E. Study of Plasmon Structure in XPS Spectra of Silver and Gold. *J. Phys. F: Met. Phys.* **1983**, *13* (1), 215–221. https://doi.org/10.1088/0305-4608/13/1/024.

(S4) Li, X.; Zhang, Z.; Henrich, V. E. Inelastic Electron Background Function for Ultraviolet Photoelectron Spectra. *J. Electron Spectros. Relat. Phenomena* **1993**, *63* (3), 253–265. https://doi.org/10.1016/0368-2048(93)87007-M.

(S5) Holzwarth, U.; Gibson, N. The Scherrer Equation versus the "Debye-Scherrer Equation." *Nature Nanotech.* **2011**, *6* (9), 534–534. https://doi.org/10.1038/nnano.2011.145.

(S6) Giordano, F.; Trovarelli, A.; de Leitenburg, C.; Giona, M. A Model for the Temperature-Programmed Reduction of Low and High Surface Area Ceria. *J. Catal.* **2000**, *193* (2), 273–282. https://doi.org/10.1006/jcat.2000.2900.